FERMILAB-CONF-13-312-AD

Physics and Applications of High Brightness Beams Workshop, HBEB 2013

Beam-Dynamics Simulations for Channeling Radiation Electron Source

D. Mihalcea[a,*], C. A. Brau[b], B. K. Choi[b], W. Gabella[b], J. D. Jarvis[c], J. W. Lewellen[d], M. Mendenhall[b], P. Piot[a,e]

[a]*Northern Illinois University, DeKalb, IL 60115, USA*
[b]*Vanderbilt University, Nashville, TN 37235, USA*
[c]*Advanced Energy Systems, Medford, NY 11763, USA*
[d]*Naval Postgraduate School, Monterey, CA 93943, USA*
[e]*Fermi National Accelerator Laboratory, Batavia, IL 60510, USA*

Abstract

The intensity and the brilliance of the compact X-ray sources based on channeling radiation are strongly dependant on the electron beam quality. It was recently proposed to combine a field-emission electron source with channeling radiation through a diamond crystal to produce high-spectral-brilliance X-rays. There are two experiments in preparation at Fermilab to prove this technique. The beam energy in the two cases are 5-MeV and 40-MeV respectively. The field-emitted beams have emittance in the nanometer range when the microbunch is 25 ps long and the charge is about 2.5fC. RF guns operating at 1.3 GHz can produce trains of at least 2×10^5 microbunches. In this contribution we present beam-dymamics simulations of a the field-emission and subsequent accelerator up to the channeling-radiation target.
© 2013 The Authors. Published by Elsevier B.V.
Selection and peer-review under responsibility of the scientific committee of HBEB 2013.

Keywords: x-ray source ; channeling radiation ; field-emission
PACS: 61.85.+p ; 85.45.Db ; 52.65.Rr

1. Introduction

One promising way to produce compact coherent high-brilliance X-ray sources is through the mechanism of channeling radiation (CR). Channeling radiation is produced when electron (or positron) beams pass through a crystal parallel with one of the crystallographic planes (1). Electrons may oscillate around that plane and produce CR, typically in X-ray range, which propagates in the same direction as the incident beam. Experimental evidence of CR was first reported in Ref. (2; 3; 4) and since this technique became a primary candidate for X-ray sources more in depth studies followed (5; 6; 7; 8).

* Corresponding author. Tel.: +01-630-840-4946
E-mail address: mihalcea@fnal.gov

1875-3892 © 2013 The Authors. Published by Elsevier B.V.
Selection and peer-review under responsibility of the scientific committee of HBEB 2013.

Operated by Fermi Research Alliance, LLC under Contract No. De-AC02-07CH11359 with the United States Department of Energy.

The properties of the incoming electron beam determine some important outgoing CR's characteristics. For example the frequency of the CR scales as $\omega = 2\gamma^2\omega_0/(1+\gamma^2\theta^2)$ where ω_0 depends on crystal lattice, γ is the Lorentz relativistic factor of the incident beam and θ is the observation angle. For moderate electron beam energy (4 to 50 MeV) the frequency of the CR is in the X-ray range. The availability of relatively small electron accelerators for this energy range translates into compactness of the X-ray source.

Although an accurate description of the CR can be made only within quantum mechanics framework, some of the classical interpretations are still valid and offer an intuitive understanding of the incident electron beam requirements. In the classical limit the electrons oscillate quasi harmonically around the crystal planes. Since the electron oscillation amplitude is limited by the interplanar distances, the kinetic energy associated with the transverse motion can be related to the maximum potential energy V_{max}. Therefore, the divergence angle of the incident electrons is limited by a critical channeling angle also related to V_{max}: $\Psi_c = \sqrt{\frac{V_{max}}{pv}}$ where p and v are electron momentum and velocity respectively (9). The value of the critical angle measured at SLAC (9), for diamond and electron beam energy of 23 GeV is 44 μrad. Since Ψ_c depends on beam energy as $\propto E^{-1/2}$ we estimate that critical channeling angle should be close to 1 mrad when beam energy is in the range 4-50 MeV.

Assuming the electron beam divergence ($\sqrt{< x'^2 >}$ same as the critical channeling angle Ψ_c, transverse beam size $\sigma_\perp$ can be related to the transverse normalized emittance $\epsilon_\perp$: $\sigma_\perp = \frac{\epsilon_\perp}{\gamma\Psi_c}$ at the focusing point (10). Since the brilliance of the X-ray source is $\propto \sigma_\perp^{-2}$, to maximize this parameter the electron beam transverse emittance should be minimized. A target brilliance of 10^{12} [photons (mm-mrad)$^{-2}$ (0.1% BW)$^{-1}$ s^{-1}] can be achieved at Fermilab Advanced Superconducting Test Accelerator (ASTA) if the beam transverse emittance is $\sim$ 1 nm (11) for 1 pC electron bunches. This emittance is much lower compared with what can be obtained with conventional cathodes. Therefore we propose to use single field emitter cathodes which can provide both the target current and beam transverse emmittance.

In this paper we present briefly the field emission cathodes manufactured at Vanderbilt University and then focus on beam dynamics simulations.

2. Field Emission Cathodes

Electrons can be extracted from a crystal through quantum tunneling process in the presence of an external electric field (12). Cathodes built on this principle are very promising for accelerator technology because they can sustain a large peak current ($\sim$ 10 A), eliminate the need for expensive laser systems and more importantly the beam emittance can be lowered to nanometer level (13). Field emission cathodes can consist either of a field emitter array when peak current must be high or just a single field emitter when very low emittance is needed.

The external electric field needed to trigger the quantum tunneling must be of the order of several GV/m. To achieve such a high electric field grounded sharp needles are placed in the vicinity of a flat gate electrode (Fig. 1). The electric field at the gate is typically about 100 A and in the region of the tip, where field emission occurs, can reach several GV/m's due to geometrical field enhancement.

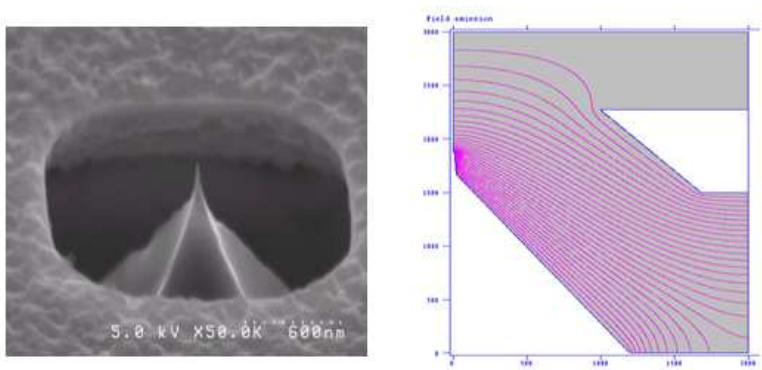

Fig. 1. Left: gated field emitter fabricated at Vanderbilt University. Right: Potential distribution around the field emitter evaluated with LANL Poisson software. The field emitter is grounded and the gate potential is 70 V.

Our field emission cathodes are fabricated at Vanderbilt Institute for Nanoscale Science and Engineering. They are made of diamond and can be either arrays or single field emitters, gated or ungated (14; 15). The field distribution around the field emitters was evaluated with LANL Poisson code (16).

Figure 1 shows a gated single field emitter (left) and the potential distribution evaluated with Poisson (right). The curvature radius of the tip is 5 nm and the gate voltage was set at 70 V. The enhancement factor defined as the ratio between the field intensity at the tip and the average field at the gate is $\beta \approx 30$. Throughout this analysis we assume that field emitters are cylindrically symmetric.

The cathode consisting of a single or multiple field emitters, gated or ungated, is typically immersed into a standard RF gun. The gate electrode is used to block the field emitted electrons with a large divergence and also to control the field emission time like, for example, in Ref. (17). In the absence of the gate electrode, field emission process is entirely controlled by the external RF field. Although the electric field at the emitter has a time dependence scaled by the RF period ($\sim$ 1 ns) it is reasonable to use the static field approximation because the time constants to reach the steady state inside the emitter are in subpicosecond range (13).

DC tests of the field emitters we intend to use to produce CR were performed at Vanderbilt University. It was measured a field emitted current of about 10 μA (from a single ungated emitter) when the external average field was 15 MV/m (18). In the RF guns at Fermilab peak electric field at the cathode can reach 40 MV/m at 1.3 GHz frequency. Since the field emission is estimated to last for about 25 ps during each RF bucket, the electric charge of each microbunch obtained from a single ungated emitter can be as high as 2.5 fC.

3. Beam Simulations

Simulations of electron beams obtained from field emitters are difficult to perform because typical distances (or simulation time steps) are in a very large range. In the vicinity of the field emitter tip simulation time step should be smaller than the curvature radius which is typically in the nanometer range. When the electrons pass the gate electrode the simulation time step can be increased to millimeter range.

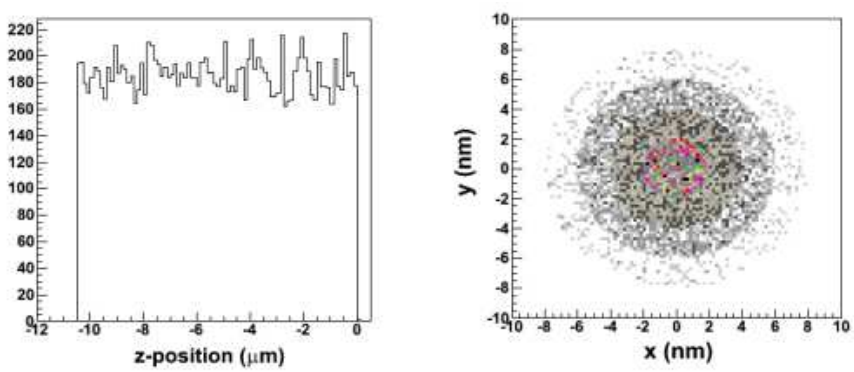

Fig. 2. Phase space projections of the initial particle distribution. Left: 25 ps long uniform longitudinal distribution. Right: transverse initial particle distribution. Particle density is determined by the external field intensity.

The beam dynamics simulations were performed with Impact-T particle in cell (PIC) code (19). Particles are tracked with Impact-T from just underneath the emitting surface through the whole injector. The initial particle distribution should take into account the field emission process. The transverse charge distribution is determined as a function of the external field intensity by using the FN equation. The field map (depicted in Fig. 1) is used to determine the electric field just outside the emitting surface in a specified number of concentric circular zones centered on the tip apex. In the case shown in Fig. 2 there are four zones with radii: 2, 4, 6 and 8 nm. Inside each zone particle distribution is constant. The longitudinal particle distribution is constant and its duration is 25 ps. We also considered truncated longitudinal gaussian distributions. The initial emittance is zero and each particle has a small longitudinal momentum of 0.3 eV.

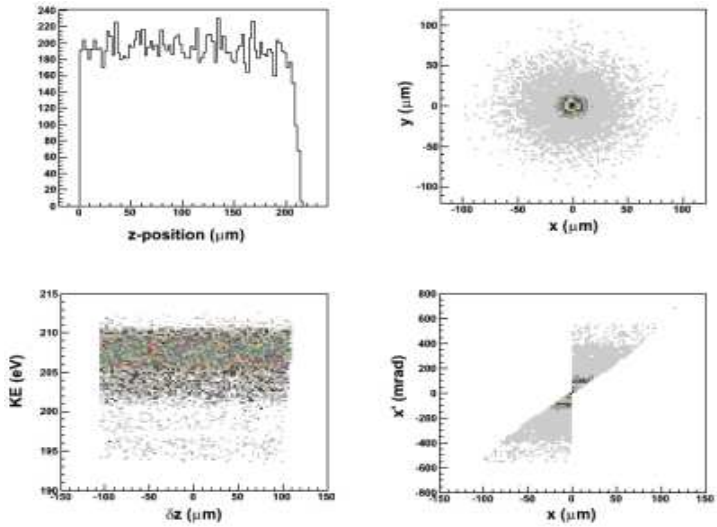

Fig. 3. Phase space projections of the particle distribution where the last emitted particle is one micron past the gate.

In the first stage of the beam dynamics simulations the initial particle distribution is moved just across the gate. Some phase space projections of the particle distribution are shown in Fig. 3 recorded when the last emitted particle is one micron past the gate. The field map resolution is 1.0 nm in the transverse plane and 0.55 nm in the longitudinal direction. In this stage the simulation time step is 1 fs.

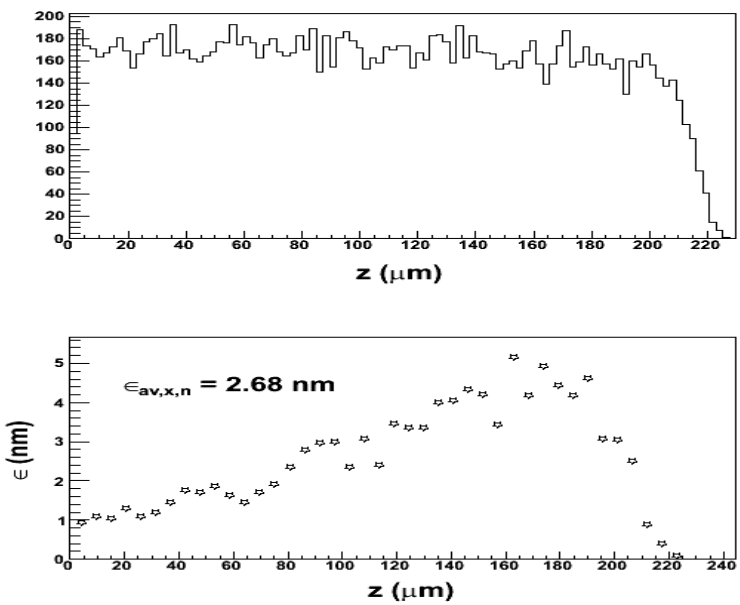

Fig. 4. Normalized transverse emittance evaluation. Longitudinal particle distribution (top) was divided into 41 slices and emittance was evaluated inside each slice (bottom).

The Impact-T code was slightly modified to turn on the 3D space charge algorithm once the particles cross the rounded field emission surface. Since the relevant output of the simulation consists of the particle distribution at a certain time step (instead of a given z-position) the longitudinal charge distribution was divided into a large number of slices and the normalized transverse emittance was evaluated from particle positions and momenta inside each slice Fig. 4. The average normalized transverse emittance is 2.7×10^{-9} m. The emittance evaluated through this procedure

should be assigned to the longitudinal position $z = 110\mu$m from the gate which corresponds to the middle of the electron bunch at the exit from the field emission structure.

The relatively large normalized emittance is primarily due to the nonlinear radial field dependence. Space charge only increases the emittance by less than 1 % for 2.5 fC microbunches.

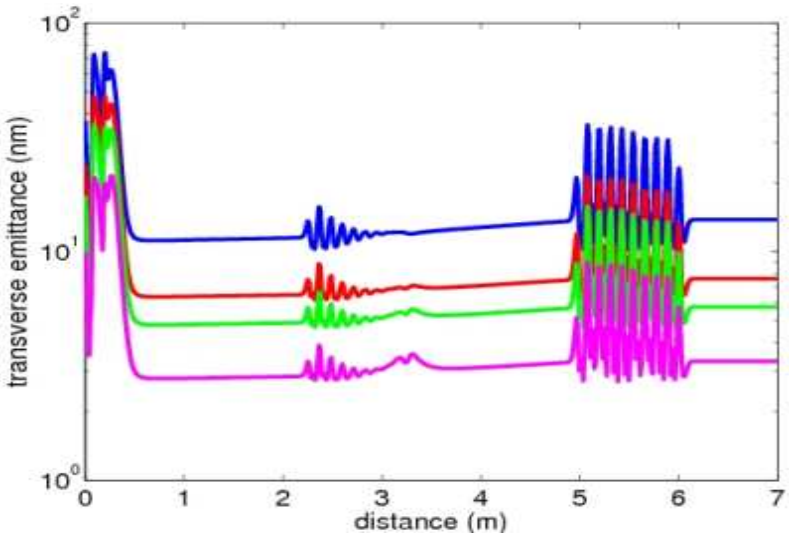

Fig. 5. Normalized transverse emittance along ASTA beamline when a certain fraction of the beam is taken into account: blue 100%, red 95%, green 90% and purple 85%.

Evaluation of the normalized emittance can be also performed by projecting the transverse coordinates at a certain z-position provided that external fields and space charge are negligible in that region. When normalized transverse emittance is evaluated just after the gate (RF gun entrance) it is 3.9^{-11} m, significantly lower than the value estimated at $z = 110\mu$m from the gate. The reason for this large discrepancy is the emittance growth in the low energy regime due to electron bunch drift (20). To minimize the effect of the emittance growth due to drift it is important to align the field emission cathode with the RF gun backplane within a few microns.

The moderate energy ($\sim$ 40 MeV) CR experiment will be conducted at Fermilab ASTA (21). The relevant portion of the beamline consists of a 1.3 GHz RF gun, two solenoids and two accelerating cavities. The longitudinal position dependence of the normalized transverse emittance is shown in Fig. 5. In this case the initial particle distribution is the output from the field emission structure (Fig. 3) with normalized emittance $\epsilon_{x,n} = 2.7 \times 10^{-9}$ m. The normalized emittance for the full beam at the experimental region located at about 10 m from the cathode only modestly increases to about 10^{-8} m.

Under the present DARPA contract there will be two experiments on channeling radiation at Fermilab. The medium energy electron beam experiment, already mentioned before, will be conducted at Fermilab ASTA injector. The second one, low energy beam ($\sim$ 4 MeV), will take place at High Brightness Electron Source Laboratory (HBESL) Fermilab facility.

The beamline at HBESL consists essentially of an RF gun, three solenoids for beam focusing and emittance compensation, a 1.3 GHz deflecting cavity for longitudinal phase space measurements and several quads for beam focusing. Spot size at the diamond crystal can be made as low as 2.8μm and the emittance can be maintained within 10^{-8} m for 25 fC electron bunches (Fig. 6).

4. Beam Parameters for Channeling Radiation Experiments

The anticipated beam and beamline parameters for both ASTA and HBESL are summarized in Table 1. For comparison purposes a column with HBESL standard photocathode parameters was also included.

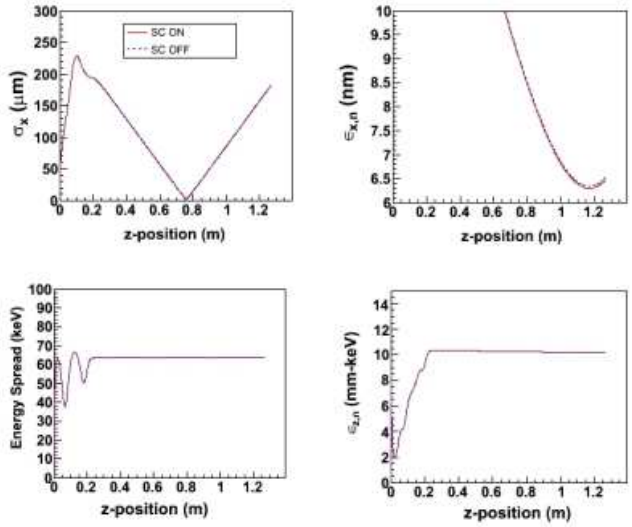

Fig. 6. Phase space projections along the HBESL beamline.

Table 1. Anticipated beam parameters for HBESL with standard photocathode, HBESL and ASTA with field emitters.

Parameter	HBESL (photocathode)	HBESL (field emitter)	ASTA (field emitter)
Cathode	CsTe	Diamond single emitter	Diamond single emitter
Macropulse current (nA)	20,000	200	200
Macropulse duration (ms)	0.4	0.4	1.0
Beam energy (MeV)	4.5	4.5	38
Emittance (nm)	4000	3	3
Spot size (nm)	450000	2800	350
Photon energy (keV)	-	2.3	85
Macropulse brilliance (/sr-s)	1×10^4	1×10^8	1×10^{11}
Macropulse flux (/sr-s)	5×10^{11}	5×10^9	5×10^{11}
Detector	Ross filter	Spectrometer	Spectrometer

The beamline construction is underway for both experiments. At HBESL the cathode will consist of a single ungated field emitter. The field emission process will be triggered by the RF gun peak electric field (~ 40 MV/m). At ASTA the CR experiment will be carried out with both gated and ungated single field emitter cathodes.

The beam parameters shown here depend strongly on the alignment accuracy between the single field emitter and the injector beam axis. Our simulations show that a displacement of 100μm between the field emitter and the beam axis would cause an emittance growth of 100%.

5. Conclusions

Single field emitter cathodes are appealing electron sources for compact X-ray devices based on CR because they can produce electron beams with normalized transverse emittance as low as a few nanometers. Our simulations also show that the emittance is essentially preserved along the whole linac. Also, the contribution of the space charge to the emittance growth is less than 1%.

Although the charge carried by each microbunch is of the order of a few fC's the total macropulse charge can be as high as ~ 200 pC because at least 200k consecutive RF buckets can be filled up during the 1 ms long macropulse. It is still an open question what is the lifetime of the field emitters operated under these conditions.

Acknowledgements

This work was supported by the DARPA Axis program under contract AXIS N66001-11-1-4196 with Vanderbilt University and Northern Illinois University. We are thankful to R. A. Carrigan, Jr. for useful discussions on channeling radiation and to M. Church and V. Shiltsev for their support.

References

[1] Lindhard J., 1964., Phys. Lett., 12, 126.
[2] Terhune R. W. and Pantell R. H., 1997. Appl. Phys. Lett., 30, 265.
[3] Gary C. K., Pantell R. W., Özcan M., Piestrup M. A. and Boyers D. G., 1991. J. Appl. Phys., 70, 2995.
[4] Klein R. K, et al, 1985. Phys. Rev. B 31, 68.
[5] Andersen J. U., Bonderup E., Pantell R. H., 1983. Ann. Rev. Nucl. Sci. 33, 453.
[6] Gevorgian L. A., Ispirian K. A., Ispirian R. K., Nucl. Instr. Meth. B, 1998. 145, 155.
[7] Carrigan R. A., Freudenberger J., Fritzler S., Genz H., Richter A., Ushakov A., Zilges A. and Sellschop J. P. F, 2003. Phys. Rev. A 68, 062901.
[8] Wagner W., Azadegan B., Sobiella M., Steiner J., Zeil K. and Pawelke J., 2007. Nucl. Instr. Meth. B 266, 327.
[9] Noble R., Seryi A., Spencer J., Stupakov G., 2009. 4th Crystal Channeling Workshop, CERN, March 27.
[10] Piot P., Brau C. A., Gabella W. E., Choi B. K., Jarvis J. D., Lewellen J. W., Mendenhall M. H., Mihalcea D., 2010. Proceedings of the 2010 Advanced Accelerator Concepts Workshop, June 10-15, Annapolis, MD, USA.
[11] Brau C. A., Choi B. K., Jarvis J. D., Lewellen J. W., Piot P., 2012. Synchrotron Radiation News 25 (1), 20.
[12] Fowler R. H., Nordheim L., 1928. Proceedings of the Royal Society of London, 119, 173.
[13] Dehler M., Candel A. and Gjonaj E., 2006. J. Vac. Sci. Tecnol. B, 24(2), 892.
[14] Choi B. K., Jarvis J. D., Brau C. A., 2012. Proceedings of the ICFA Workshop on Future Light Sources, Jefferson Lab, Newport News, Virginia, USA.
[15] Jarvis J. D., Andrews H. L., Brau C. A., Choi B. K., Davidson J., Kang W. P., Wong Y. M., 2009. Journal of Vacuum Science & Technology, B 27, 2264.
[16] Billen J. H. and Young L. M., LANL report LA-UR-96-1834.
[17] J. W. Lewellen J. W. and J. Noonan J., 2005. Pysical Review Special Topics - Accelerators and Beams, 8, 033502.
[18] Gabella W. E., Brau C. A., Choi B. K., Ivanov B., Jarvis J. D., Mendenhall M. H., Piot P., Mihalcea D., Carrigan R., Wagner W., 2012. Submitted to Nucl. Inst. Meth. B.
[19] Qiang J., et al., 2006. Proceedings of 2005 IEEE Particle Accelerator Conference (PAC 05), Knoxville TN, 3316.
[20] Floetmann K., 2003. Physical Review Special Topics - Accelerators and Beams, 6, 034202.
[21] Nagaitsev S. and Piot P., 2007. Proccedings of PAC07, 2942.